Level-dependent volatility in jumping short-rate models

Nigel Elton Nyasha Chitambo

A dissertation submitted to the Faculty of Commerce, University of Cape Town, in partial fulfilment of the requirements for the degree of Master of Philosophy.

October 4, 2024

MPhil in Mathematical Finance,
University of Cape Town.

Declaration

I declare that this dissertation is my own unaided work. It is being submitted for the Degree of Master of Philosophy at the University of Cape Town. It has not been submitted before for any degree or examination in any other University.

October 4, 2024

CHTNIG001

Nigel Elton Nyasha Chitambo

Signed by candidate

Abstract

This dissertation constructs a no-arbitrage term structure with deterministically timed randomly sized jumps to price interest rate contingent claims while accounting for level-dependent volatility. This dissertation will price such claims using an implicit finite difference scheme to implement a modelling framework that prices bonds, bond options and caplets with scheduled shocks to the short-term interest rate to simulate macroeconomic announcements and other sudden developments. This dissertation found that the prices derived from the implicit finite difference scheme agree with those derived from Monte-Carlo simulations and, where applicable, analytical solutions. Moreover, this dissertation shows how innovations in the short-term rate affect the valuations of interest rate contingent claims.

Acknowledgements

"What seems to us as bitter trials are often blessings in disguise for which we are later, in the fullness of time and understanding, very grateful for!" – Oscar Wilde

I am deeply indebted to Dr. Alex Backwell for his patience, counsel and support throughout this dissertation process.

I would like to extend my sincere thanks to AIFMRM for affording me this opportunity.

Moreover, I would be remiss in not mentioning my family and friends, who have waited earnestly for this day. Thank you for your belief in me; it kept me going.

Finally, I would like to thank God for the strength provided.

Contents

List of Figures

List of Tables

Chapter 1

Introduction

We concern ourselves with floating-rate liabilities, which create significant unpredictability for borrowers when assessing their debt obligations. In an environment beset with looming interest rate hikes, interest derivatives such as caps offer a ceiling on the interest charge for such liabilities. They are constituted by a series of caplets, call options on an interest rate, and will be the focus of this dissertation. We seek to provide a framework for numerically pricing interest rate contingent claims by implementing a finite-difference algorithm where the underlying short-rate process has mean-reverting diffusion, a jump component, and level-dependent volatility.

The literature surrounding factor jump models is extensive (Baz and Das, 1996; Das, 1996; Johannes, 2004; da Silva, Baczynski and Vicente, 2016; Backwell and Hayes, 2022). These models augment those of Vasicek (1977) and Cox *et al.* (1985) with a jump-diffusion to admit discontinuities in the underlying interest process. The inclusion of jump-diffusions in canonical short-rate models is motivated by market crashes (Das, 1996), scheduled macroeconomic announcements (Kim and Wright, 2014) and policy surprises (Bauer, 2014).

Das (1996) employs a finite-difference approach to solve a partial differential-difference equation to compute the price of bonds and options. Baz and Das (1996) then provide a closed-form approximation for bond prices. However, these approaches only consider the case of unexpected jumps.[1] Kim and Wright (2014) present a closed-form approximation for bond prices where jumps are expected (i.e., have a deterministic timing, but not usually a deterministic size), and Backwell and Hayes (2022) provide a finite-difference implementation for pricing bonds and caplets in the context of expected and unexpected jumps. Our approach develops on the work of Kim and Wright (2014) by providing a numerical implementation, and our procedure is comparable to Backwell and Hayes (2022) but is limited to the

[1] Unexpected jump arrivals are governed by a Poisson process, with some intensity. Simply put, unexpected jumps occur at random times.

context of expected jumps and a single state variable ($r(t)$).[2]

Backwell and Rudd (2023) present an empirical approach to measuring level-dependent volatility, the notion of a positive relationship between interest-rate changes and interest-rate volatility changes.[3] By juxtaposing interest rates and cap-floor volatilities in the South African market, they scrutinise the idea that interest rate volatility has positive level-dependence and find that the effect of level-dependence decreases as interest rates increase. Our study specifies linear functions for the short-rate and jump volatility to mimic the effect of level-dependence.

Rebonato (2004) provides a historical context for the shapes of interest-rate smiles. Significant changes were observed during the 1990s; over the decade, interest rate smiles would evolve from being typically flat across all strikes to having more pronounced smiles around 1994 (Rebonato, 2004, Ch.7, p.223).

Furthermore, the cessation of LIBOR and the growing interest in alternative benchmarks has sparked considerable discourse among market participants concerning, but not limited to, collateral discounting, interest rate derivative markets, precessation triggers, and bilateral trading (Lyashenko and Mercurio, 2019; Schrimpf and Sushko, 2019; Andersen and Bang, 2020; Piterbarg, 2020). Lyashenko and Mercurio (2019) goes on to contrast the valuation of caplets under forward and backward-looking risk-free reference rates (RFRs), noting that for an accrual period $[T_{i-1}, T_i)$ in both cases, the lognormal forward rate $F(t, T_{i-1}, T_i)$ still has a dependency on the T_i-forward measure. Using the tower property of conditional expectation and Jensen's inequality, Lyashenko and Mercurio (2019) demonstrates that the forward-looking caplet is cheaper than its backward-looking counterpart, with a similar relationship arising when comparing implied volatilities. This dissertation engages in this discourse by modelling the effect of scheduled macroeconomic announcements on the yield curve and interest rate options (Kim and Wright, 2014) in a forward-looking setting.

Figure 1.1 shows a 2021-2024 time series of two significant interest rate benchmarks in the Sterling market, the Sterling Overnight Index Average (SONIA) and the GBP 3-month Overnight-Index Swap (OIS) rate. The Bank of England's (BoE) Monetary Policy Committee (MPC) publishes its Monetary Policy Report (MPR) quarterly. They use this report to make decisions regarding the Bank Rate, which then influences other interest rates in the Sterling market as they follow each other closely. The jumps exhibited by SONIA on the MPR publication dates form the motivation for our model, and we will later assume that jumps occur quarterly.

[2] Expected jump arrivals are governed by a deterministic counting process, giving off the effect that jumps occur at known times.

[3] Interest-rate volatility is high when interest rates are high.

Backwell and Hayes (2022) consider a period from 2016-2020 and note that for the benchmarks in Figure 1.1, upcoming MPC announcements are anticipated by three-month rates. Backwell and Hayes (2022) introduce an auxiliary state variable to capture the size of the jump; however, this dissertation will consider a single curve framework and only a single state variable, namely the short-rate.

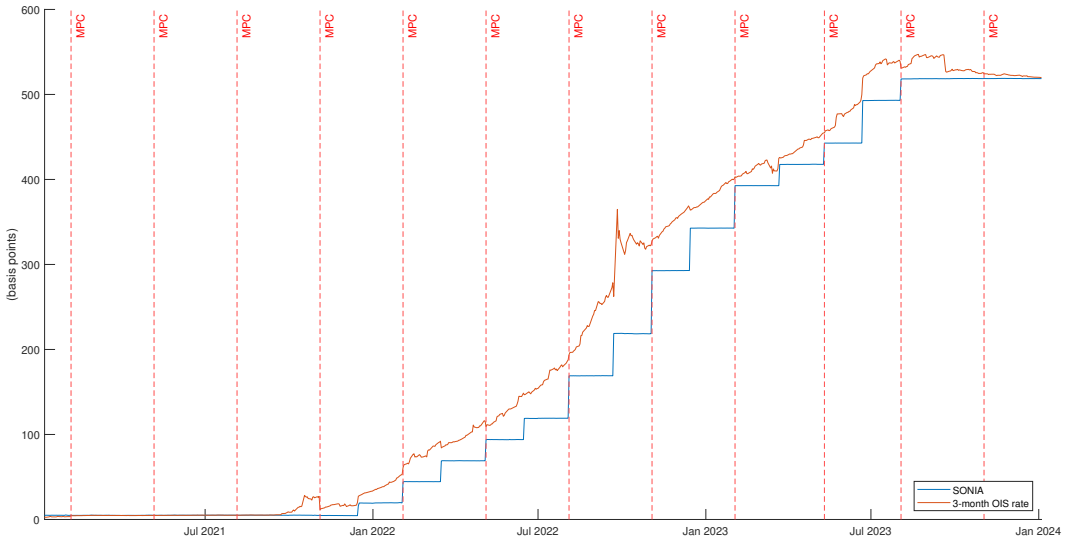

Fig. 1.1: A three-year history of interest rates in the key Sterling market. The dashed vertical lines delineated by 'MPC' indicate the report publication dates.

Given the background of the literature, the aim of this dissertation is twofold. First, we price caplets using finite-difference methods in the context of expected jumps while the short-rate and jump volatility increase with the level of the short-rate. Finally, we demonstrate how implied volatility skews change shape as level-dependence increases. The more dependent volatility is on the short-rate level, the steeper the volatility skew. We compute implied volatility using both Black's (Black, 1976) and Bachelier's (Bachelier, 1900) formulae, thus under different assumptions of the forward-term rate, and observe the impact. Black's formula assumes a log-normal distribution for the dynamics of the forward-term rate and accounts for level-dependence, whereas Bachelier's formula assumes a normal distribution (no level-dependence).

The dissertation will take on the following structure. In Chapter 2, the general class of models under consideration is introduced. In Chapter 3, our focus shifts to a specific instance of a model introduced in Chapter 2. We outline a framework for numerically pricing interest rate contingent claims and computing implied volatility under different assumptions of a forward-looking term rate. To price caplets in this framework, we begin with zero-coupon bonds and then bond options. Chapter 3

outlines a framework for numerically pricing interest rate contingent claims and computing implied volatility under different assumptions of a forward-looking term rate. In Chapter 4, we discuss the effects of each parameter of our model in isolation. Chapter 5 concludes the dissertation.

Chapter 2

Model

This section introduces the class of models used throughout the dissertation; we provide a nested generalisation of the short-rate model presented in Kim and Wright (2014).

2.1 Data

The data is sourced from Refinitiv Eikon, and we consider a three-year period from January 2021 to January 2024. We contrast the Bank Rate, Sterling Overnight Index Average (SONIA) and the GBP 3-month Overnight-Index Swap (OIS) rate against one another in Figure 1.1. The MPC meeting dates were procured from the Bank of England's website.

2.2 Short-rate model with deterministic jumps

We assume a risk-neutral measure exists, denoted $\mathbb{Q}$. Suppose that the following process governs the short-rate:

$$dr(t) = \kappa(\theta - r(t))dt + (\sigma_r + \alpha r(t))dW(t)^{\mathbb{Q}} + J(t)dN(t), \tag{2.1}$$

$$J(t) \overset{\mathbb{Q}}{\sim} \mathcal{N}(\mu, (\sigma_J + \beta r(t))^2), \tag{2.2}$$

where κ, θ, σ_r, α, μ, σ_J and β are constants. Parameter κ represents the speed of mean-reversion, θ the is mean reversion level, $\sigma_r + \alpha r(t)$ is the instantaneous absolute volatility of the short-rate, $J(t)$ is the deterministic jump with mean μ and standard deviation $\sigma_J + \beta r(t)$, $W(t)^{\mathbb{Q}}$ is a standard Brownian motion under the risk-neutral measure, and $N(t)$ is a deterministic counting process defined as follows:

$$N(t) = \sum_{s \geq 1} \mathbb{1}_{[t_s, \infty)}(t), \quad t \geq 0 \ ,$$

where

$$\mathbb{1}_{[t_s,\infty)}(t) = \begin{cases} 1, & \text{if} \quad t \geq t_s, \\ 0, & \text{if} \quad 0 \leq t < t_s, \end{cases}$$

with $s \geq 1$ and $\mathcal{T}_J = \{t_1, t_2, \ldots, t_s, \ldots, t_n\}$ as a collection of deterministic jump times.

Market practitioners often quote caplet prices in terms of the implied volatility. The volatility skew, a plot of implied volatility across different strike levels, captures the market's view of the volatility of the underlying forward rates (Rebonato, 1996). Market participants will have their expectations and sentiments regarding the level and volatility of interest rates shaped by anticipated macroeconomic announcements and other sudden developments.

In (2.1) and (2.2), the degree of level-dependence is specified through parameters α and β, respectively.[1] Precisely, α controls the level-dependence of the Brownian-motion part of the model, whereas β controls the level-dependence of the jump part.

- Assuming no jumps occur and $\alpha = 0$ (no level-dependence), (2.1) reduces to the canonical Vasicek (1977) short-rate model with constant volatility.
- Assuming that jumps occur and $\alpha = \beta = 0$ (no level-dependence), (2.1) and (2.2) reduces to the Kim and Wright short-rate model with constant volatilities in the short-rate component and the jump component.
- Varying α allows us to impose different gradations of level-dependence on the short-rate model. We have positive level-dependence when $\alpha > 0$ and negative level-dependence when $\alpha < 0$.[2]
- Varying β allows us to impose different gradations of level-dependence on the jump component. We have positive level-dependence when $\beta > 0$ and negative level-dependence when $\beta < 0$.[3]

Table 2.1 shows two special cases of the model in (2.1) and (2.2).

[1] The degree to which the short-rate volatility depends on short-rate levels.

[2] Short-rate volatility is higher when short-rates are high. Short-rate volatility is lower when short-rates are high.

[3] Jump size volatility is higher when short-rates are high. Jump size volatility is lower when short-rates are high.

Model	Dynamics	κ	θ	α	μ	β
Vasicek (1977)	$dr(t) = \kappa(\theta - r(t))\,dt + \sigma_r\,dW(t)^{\mathbb{Q}}$	-	-	0	0	0
Kim and Wright (2014)	$dr(t) = \kappa(\theta - r(t))\,dt + \sigma_r\,dW(t)^{\mathbb{Q}} + J(t)\,dN(t)$	-	-	0	-	0

Tab. 2.1: Summary of short-rate models.

2.3 Contingent claims

We now turn our attention to European contingent claims. Here, we will provide prototypical payoffs of such claims. Letting H_T denote a general payoff at time T, the time-t stochastic discount factor is given by $D(t,T) = \exp\left(-\int_t^T r(u)du\right)$ and the time-t price of the claim is given by:

$$V(t,T) = \mathbb{E}^{\mathbb{Q}}\left[\exp\left(-\int_t^T r(u)du\right)\ H_T \mid \mathcal{F}_t\right] \tag{2.3}$$

$$= \mathbb{E}^{\mathbb{Q}}\left[D(t,T)\ H_T \mid \mathcal{F}_t\right]. \tag{2.4}$$

2.3.1 Zero-coupon bond

Let the time-t price of a zero-coupon bond maturing at time T be denoted $P(t,T)$. At maturity, it pays the holder one unit of currency. The price is given by

$$P(t,T) = \mathbb{E}^{\mathbb{Q}}\left[D(t,T)\ H_T^{\text{ZB}} \mid \mathcal{F}_t\right] \tag{2.5}$$

$$= \mathbb{E}^{\mathbb{Q}}\left[D(t,T) \mid \mathcal{F}_t\right], \tag{2.6}$$

where $H_T^{\text{ZB}} := 1$.

2.3.2 Bond option

Let $V(t,T)$ denote the value of a T-year European bond option paying $H^{\text{ZBO}}[P(T,S)]$ at expiry. The strike of the option is given as P_K, and the underlying bond $P(T,S)$ denotes the value of a zero-coupon bond maturing at time S, where $S > T$. Then $H^{\text{ZBO}}[P(T,S)] := \max\left[\omega(P(T,S) - P_K), 0\right]$ and (2.4) becomes

$$V(t,T) = \mathbb{E}^{\mathbb{Q}}\left[D(t,T)\ H^{\text{ZBO}}[P(T,S)] \mid \mathcal{F}_t\right] \tag{2.7}$$

$$= \mathbb{E}^{\mathbb{Q}}\left[D(t,T)\ \max\left[\omega(P(T,S) - P_K), 0\right] \mid \mathcal{F}_t\right], \tag{2.8}$$

where we set $\omega = 1$ for calls and we set $\omega = -1$ for puts.

2.3.3 Caplet and floorlet

For caplets on an underlying rate L struck at K over tenor δ, we have $H^{\text{Caplet}}(L) = \delta\max[\omega(L-K),0]$ and

$$V(t,T) = \mathbb{E}^{\mathbb{Q}}\left[D(t,T)\ H^{\text{Caplet}}(L) \mid \mathcal{F}_t\right], \tag{2.9}$$

for $\omega = 1$ we have caplets and for $\omega = -1$ we have floorlets. Note that caplet and floorlet prices can be expressed in terms of bond option prices; see Appendix A.

2.4 Closed-form solution for bond prices

The second entry of Table 2.1 (where $\alpha = \beta = 0$) refers to the work done by Kim and Wright (2014). They demonstrate that bond prices can be expressed as follows:

$$P(t,T) = \exp\left(A(t,T) + B(t,T)r(t)\right), \tag{2.10}$$

where

$$\tilde{A}(t,T) = \left(\frac{\sigma^2}{2\kappa^2} - \theta\right)[(T-t) + B(t,T)] - \frac{\sigma^2}{4\kappa}A^2(t,T)$$

$$A(t,T) = \tilde{A}(t,T) + \sum_{t<t_s<T}\left(-\frac{1}{\kappa}[1-e^{-\kappa(T-t_s)}]\mu + \frac{\nu^2}{2\kappa^2}(1-e^{-\kappa(T-t_s)})^2\right)$$

$$B(t,T) = \frac{1}{\kappa}\left(e^{-\kappa(T-t)} - 1\right),$$

furthermore, $\mathcal{T}_J = \{t_1, t_2, \ldots, t_s, \ldots, t_n\}$ is a family of jump times.

Deterministic functions A and B do not depend on t and T individually, but only on the difference $T-t$, i.e., the time to maturity. The drift and volatility-squared of Kim and Wright's model are affine functions of the short-rate; thus, the short-rate model of Kim and Wright (2014) is an affine term structure model (Duffie and Kan, 1996).

Chapter 3

Numerical procedure

This section considers the generalised model (2.1) discussed in the previous chapter. We now describe the numerical implementation and develop a framework using an implicit finite-difference scheme to price interest-rate contingent claims. The jumps in (2.1) will correspond to quarterly macroeconomic announcements, and an appropriate jump condition will be imposed on the finite-difference scheme. This section then benchmarks the performance of this finite-difference scheme against a Monte-Carlo procedure.

3.1 Finite-difference implementation

By the Feynman-Kac Theorem (see e.g., Øksendal (2003, Ch.8, p.145) the contingent claim prices (2.5), (2.7) and (2.9) can be transformed into solutions of partial differential equations (PDEs). All of these pricing payoff functions are not dependent on the short rate path.[1]

This segment sets forth a framework designed to price interest rate contingent claims under a finite-difference scheme with deterministically timed jumps while accounting for level-dependent volatility.

3.1.1 Absence of jumps

First, we consider the case in which there are no jumps. Given (2.1), we can solve (3.1) to value a contingent interest rate claim. The short-rate process is Markov, so the price is given by a deterministic function $V(t,T) = V(r(t),t,T)$. As a result, we have the following:

[1] The short-rate process is Markov.

$$\begin{cases} \frac{1}{2}(\sigma_r + \alpha r)^2 \frac{\partial^2 V}{\partial r^2} + \kappa(\theta - r)\frac{\partial V}{\partial r} + \frac{\partial V}{\partial t} - rV = 0, \quad t \leq T \\ V(r, T, T) = H(r). \end{cases} \tag{3.1}$$

We now construct a uniform grid of points (t_i, r_j), $i = 0, \ldots, N$, $j = 0, \ldots, M$ where N represents the number of time-steps and M represents the number of spatial-steps such that

$$\Delta_t = \frac{t_N - t_0}{N},$$

and

$$\Delta_r = \frac{r_M - r_0}{M}.$$

By construction, there is an equal distance Δ_r between any two consecutive points in the interval $[r_0, \ldots, r_M]$ and an equal distance Δ_t between any two consecutive points in the interval $[t_0, \ldots, t_N]$. Figure 3.1 below visualises the uniform grid of points (t_i, r_j).

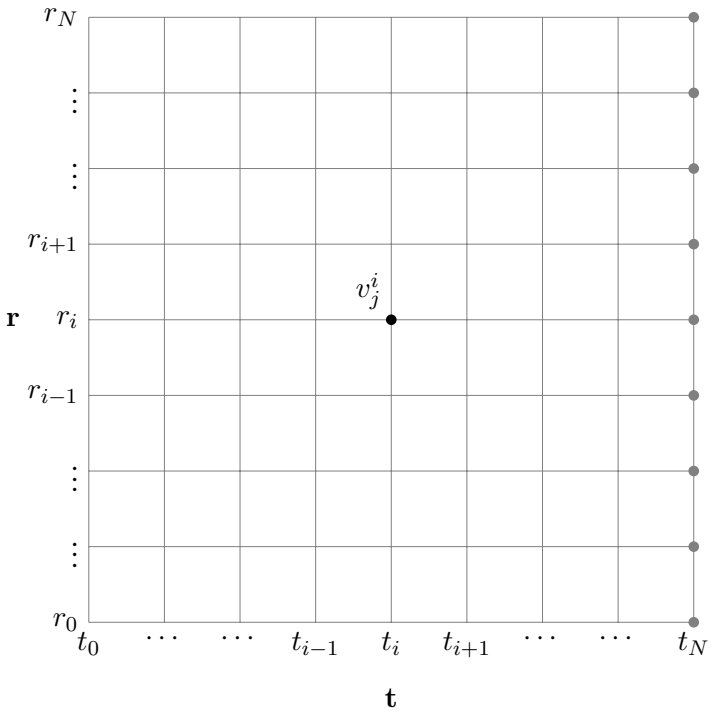

Fig. 3.1: Finite-difference grid.

The value of a contingent claim V at node (i, j) is denoted by $v(t_i, r_j) = v_j^i$. So, given an initial short-rate r_j, the time-t_i value of a contingent claim maturing at time $t_N = T$ is given as $V(r_j, t_i, t_N)$.

We approximate the derivatives in (3.1) by:

$$\frac{\partial^2 V}{\partial r^2} = \frac{v_{j+1}^i - 2v_j^i + v_{j-1}^i}{(\Delta_r)^2}, \tag{3.2}$$

$$\frac{\partial V}{\partial r} = \frac{v_{j+1}^i - v_{j-1}^i}{2\Delta_r}, \tag{3.3}$$

and

$$\frac{\partial V}{\partial t} = \frac{v_j^{i+1} - v_j^i}{\Delta_t}. \tag{3.4}$$

Substituting (3.2), (3.3) and (3.4) into (3.1) yields:

$$\frac{1}{2}(a + br_j)^2 \left(\frac{v_{j+1}^i - 2v_j^i + v_{j-1}^i}{(\Delta_r)^2} \right) + \kappa(\theta - r_j) \left(\frac{v_{j+1}^i - v_{j-1}^i}{2\Delta_r} \right) + \frac{v_j^{i+1} - v_j^i}{\Delta_t} - r_j v_j^i = 0,$$

which can be written as,

$$a_{j,j-1} v_{j-1}^i + a_{j,j} v_j^i + a_{j,j+1} v_{j+1}^i = v_j^{i+1},$$

where

$$a_{j,j-1} = -\frac{1}{2} \left(\frac{(\sigma_r + \alpha r_j)^2 \Delta_t}{(\Delta_r)^2} - \frac{\kappa(\theta - r_j)\Delta_t}{\Delta_r} \right),$$

$$a_{j,j} = 1 + r_j \Delta_t + \frac{(\sigma_r + \alpha r_j)^2 \Delta_t}{(\Delta_r)^2},$$

and

$$a_{j,j+1} = -\frac{1}{2} \left(\frac{(\sigma_r + \alpha r_j)^2 \Delta t}{(\Delta_r)^2} + \frac{\kappa(\theta - r_j)\Delta_t}{\Delta_r} \right).$$

Now, suppose that we can represent the above as:

$$\mathbf{A}\, \mathbf{V}_i = \mathbf{V}_{i+1},$$

where $\mathbf{A}$ is a $(M+1)\times(M+1)$ matrix:

$$\mathbf{A}=\begin{bmatrix} -1 & 2 & -1 & 0 & \cdots & \cdots & 0 \\ a_{1,0} & a_{1,1} & a_{1,2} & 0 & \cdots & \cdots & 0 \\ 0 & 0 & \ddots & \ddots & \ddots & \ddots & 0 \\ \vdots & \ddots & \ddots & \ddots & \ddots & \ddots & \vdots \\ \vdots & \vdots & \ddots & \ddots & \ddots & \ddots & 0 \\ 0 & \cdots & \cdots & 0 & a_{M-2,M-1} & a_{M-1,M-1} & a_{M-1,M} \\ 0 & \cdots & \cdots & 0 & -1 & 2 & -1 \end{bmatrix},$$

and $\mathbf{V}_i$ is a $(M+1)\times 1$ vector consisting of time-t_i values:

$$\mathbf{V}_i=\begin{bmatrix} v_0^i & v_1^i & \cdots & v_{M-1}^i & v_M^i \end{bmatrix}^\top.$$

We assume the solution near the extreme nodes of V_i (v_0^i and v_M^i) can be extrapolated as follows, using the first row of $\mathbf{A}$ to aid in the extrapolation, we have

$$\begin{aligned} v_0^i &= v_1^i-(v_2^i-v_1^i) \\ &= 2v_1^i-v_2^i, \end{aligned}$$

and using the last row, we have

$$\begin{aligned} v_M^i &= v_{M-1}^i-(v_{M-2}^i-v_{M-1}^i) \\ &= 2v_{M-1}^i-v_{M-2}^i. \end{aligned}$$

Through backward recursion from $i=N-1$ to $i=0$, we compute the value of a contingent claim as follows:

$$\mathbf{V}_i=\mathbf{A}^{-1}\mathbf{V}_{i+1},\quad i=N-1,\ldots,0, \tag{3.5}$$

where $\mathbf{V}_N$ is set according to the payoff function H.

Payoff functions and terminal conditions

By modifying the terminal condition H, we can price zero-coupon bonds, bond options and caplets. By setting $H=1$ and running (3.5) from $t=T$ to $t=0$, we can find the price of a time-$t=0$ zero-coupon bond maturing at time $t=T$.

To find the price of a put struck at V_K expiring at time T on a zero-coupon bond maturing at time S, with $S>T$; we set $H=1$ and run (3.5) from $t=S$ to $t=T$. At time $t=T$, we insert the bond price $V(r,T,S)$ into the terminal condition yielding

$H = \max(V_K - V(r, T, S), 0)$ and we run the finite-difference scheme from $t = T$ to $t = 0$.

Finally, to determine the price of a caplet; we use the same approach to pricing bond puts along with the result in Appendix A. First we set $V_K = \dfrac{1}{1 + K(S - T)}$ and we obtain caplet prices by setting the terminal condition to a multiple of a put $H = (1 + K(S - T))\max(V_K - V(r, T, S))$.

3.1.2 Presence of jumps

We now consider the case in which there are jumps. The methodology is comparable to Section 3.1.1, but we must apply special care when we arrive at a jump time through our backward recursion. Recall that we are considering fixed, given jump times, which may occur during the life of a contingent claim.

When we are at jump time $\mathcal{T}_J = \{t_1, t_2, \ldots, t_s, \ldots, t_n\}$, we insert the following jump-condition:

$$\mathbf{V}_{s^-} = V(r_s^-, t_s^-, T) = \mathbb{E}_{s^-}\left[V(r_s^+, t_s^+, T)\right]. \tag{3.6}$$

The contingent claim price immediately before the jump (at time t_s^-), is the risk-neutral expectation of the contingent claim after the jump (at time t_s^+). The right-hand side of (3.6) can be calculated by taking a (risk-neutral) expectation over the post-jump possibilities, $V(r_s^+, t_s^+, T)$, as per standard no-arbitrage pricing.

To take the expectation of the right-hand side, we temporarily extrapolate our grid (t_i, r_j) along the two most extreme nodes of our spatial variable axis r_j. The spatial variable axis r_j is then indexed from $j = -\frac{m}{2}, -\frac{m}{2} + 1, \ldots, -1, 0, 1, \ldots, M - 1 + \frac{m}{2}, M + \frac{m}{2}$.

We then insert an additional step, as follows, between the standard steps in (3.5), whenever a jump time is encountered:

$$\mathbf{V}_{\mathbf{s}^-} = \mathbb{E}_{t_s^-}\left[\mathbf{V}_{\mathbf{s}^+}\right] \tag{3.7}$$

$$\approx \mathbf{B}\mathbf{V}_{\mathbf{s}^+}, \tag{3.8}$$

where $\mathbf{B}$ is a $(M + 1) \times (M + m + 1)$ matrix containing probabilities, such that the above matrix multiplication approximately evaluates the expectation. Each row of B will contain a discrete probability distribution, which will weight the corresponding post-jump possibilities. In terms of column vectors,

$$\mathbf{B} = \begin{bmatrix} b_{*,-\frac{m}{2}} & \cdots & b_{*,j} & \cdots & b_{*,M+\frac{m}{2}} \end{bmatrix},$$

where the j-th column of $\mathbf{B}$ is denoted as $b_{*,j}$ and $m = \left\lceil 3 \times \frac{\max(\sigma_J + \beta r_i)}{\Delta_r} \right\rceil$.[2] We denote the normal cumulative density function as:

$$F(x|\mu,\sigma) = \frac{1}{\sigma\sqrt{2\pi}} \int_{-\infty}^{x} e^{-\frac{(t-\mu)^2}{2\sigma^2}}\, dt, \quad \text{for } x \in \mathbb{R}. \tag{3.9}$$

The constituents of $\mathbf{B}$ can then be expressed as:

$$\begin{aligned}
b_{i,-\frac{m}{2}} &= F(r_{-\frac{m}{2}} \,|\, r_i, \sigma_J + \beta r_i), \\
b_{i,j} &= F(r_j + \epsilon \,|\, r_i, \sigma_J + \beta r_i) - F(r_j - \epsilon \,|\, r_i, \sigma_J + \beta r_i), \quad -\frac{m}{2} < j < M + \frac{m}{2}, \\
b_{i,M+\frac{m}{2}} &= 1 - F(r_{M+\frac{m}{2}} \,|\, r_i, \sigma_J + \beta r_i),
\end{aligned}$$

and $\mathbf{V}_{\mathbf{s}^+}$ is a $(M + m + 1) \times 1$ vector:

$$\mathbf{V}_{s^+} = \begin{bmatrix} v^{s^+}_{-\frac{m}{2}} & v^{s^+}_{-\frac{m}{2}+1} & \cdots & v^{s^+}_{M-1+\frac{m}{2}} & v^{s^+}_{M+\frac{m}{2}} \end{bmatrix}^\top,$$

while $\mathbf{V}_{\mathbf{s}^-}$ is a $(M + 1) \times 1$ vector:

$$\mathbf{V}_{s^-} = \begin{bmatrix} v^{s^-}_0 & v^{s^-}_1 & \cdots & v^{s^-}_{M-1} & v^{s^-}_M \end{bmatrix}^\top.$$

The non-square matrix $\mathbf{B}$ mimics the function of a probability transition matrix such that its rows sum up to one:

$$\sum_j b_{i,j} = 1,$$

allowing us to take an expectation over the post-jump possibilities as in (3.7). In the absence of jumps, matrix $\mathbf{B}$ is square and simplifies into the identity matrix $\mathbf{I}$ of dimension $(M + 1) \times (M + 1)$.

3.2 Monte-Carlo simulation

Through Monte-Carlo simulation, we benchmark the accuracy of the above numerical scheme.

[2] The support of (3.9) covers the entire real line. We truncate this interval such that approximately 99.7% of our jump range falls within three standard deviations. This gives us a good approximation for the maximum jump size included in the grid.

We compute short-rate realisations at times $t = 0 < t_1, ... < t_N$ of (2.1) across n sample paths using the following algorithm[3]:

Algorithm 1 Contingent claim Pricing using Monte-Carlo Simulation

Input: $\kappa, \theta, \sigma_r, \sigma_J, N, T, \mathcal{T}_J$
$n \leftarrow 50000$
for $i = 0, \ldots, N-1$ **do**
    generate n i.i.d. samples from $\mathbf{Z}_1 \sim \mathcal{N}(0,1)$
  if $t_{i+1} \in \mathcal{T}_J$ **then**
    generate n i.i.d. samples from $\mathbf{Z}_2 \sim \mathcal{N}(0,1)$
    $\mathbf{r(t_{i+1})} \leftarrow \kappa(\theta - \mathbf{r(t_i)})(t_{i+1} - t_i) + \sigma_r\sqrt{(t_{i+1} - t_i)}\mathbf{Z_1} + \sigma_J\mathbf{Z}_2$
  else
    $\mathbf{r(t_{i+1})} \leftarrow \kappa(\theta - \mathbf{r(t_i)})(t_{i+1} - t_i) + \sigma_r\sqrt{(t_{i+1} - t_i)}\mathbf{Z_1}$
  end if
end for

Supplying equations (2.5), (2.7), and (2.9) as payoffs, we obtain time-$t = 0$ prices.

Given realisations of the short-rate $r(t_1), \ldots, r(t_N)$, we can compute realisations of the discount factor that corresponds to the payout of one unit of currency at time t:

$$\begin{aligned} D(0,t) &= \exp\left(-\int_0^t r(u)du\right) \\ &= \exp\left(-Y(t)\right). \end{aligned}$$

Then, by using trapezoidal quadrature, we obtain

$$Y(t_i) \approx \sum_{j=1}^{i} \frac{r(t_{j-1})(t_j - t_{j-1})}{2}.$$

3.3 Model-implied volatility framework

This section considers the model-implied volatility for a caplet under the short-rate process specified in (2.1). Model-implied volatility lets us see the variety of shapes of implied volatility these models can generate.

Definition 3.1 (Forward Rate)**.** The time-t forward rate for a period $[T_{i-1}, T_i]$ is given by

$$F(t; T_{i-1}, T_i) = \frac{1}{T_i - T_{i-1}} \frac{P(t, T_{i-1}) - P(t, T_i)}{P(t, T_i)}, \tag{3.10}$$

[3] We employ an Euler scheme, see Chapter 3 of Glasserman (2003) for a more detailed discussion.

where $t \leq T_{i-1} \leq T_i$.

Market practitioners are spoilt for choice when deriving assumptions that dictate the evolution of the forward-term rate $F(t; T_{i-1}, T_i)$.[4, 5] Traditionally, the lognormal forward-LIBOR market model assumes that the evolution of $F(t; T_{i-1}, T_i)$, under the forward measure T_i is dictated by:

$$dF(t; T_{i-1}, T_i) = \sigma_{\text{LN}}\, F(t; T_{i-1}, T_i) dW_t^{T_i},$$

where σ_{LN} refers to the implied volatility through which caplets are priced using Black's formula:

$$V_{\text{Black}}(F, \sigma, T, K, b) = b\left[F\Phi(d_1) - K\Phi(d_2)\right], \tag{3.11}$$

where

$$d_1 = \frac{\log(F/K) + \frac{\sigma^2 T}{2}}{\sigma\sqrt{T}}$$
$$d_2 = \frac{\log(F/K) - \frac{\sigma^2 T}{2}}{\sigma\sqrt{T}}.$$

Under the normal forward-LIBOR market model, $F(t; T_{i-1}, T_i)$ is governed by

$$dF(t; T_{i-1}, T_i) = \sigma_{\text{N}}\, dW_t^{T_i},$$

where σ_{N} refers to the implied volatility through which caplets are priced using Bachelier's formula:

$$V_{\text{Bachelier}}(F, \sigma, T, K, b) = b[(F - K)\Phi(d_1) + \sigma\sqrt{T}\phi(d_1))], \tag{3.12}$$

where

$$d_1 = \frac{F - K}{\sigma\sqrt{T}}.$$

To price caplets, (3.11) and (3.12), respectively, become

$$V^{\text{Caplet}}(t) = V_{\text{Black}}\left(F(t; T_{i-1}, T_i), \tilde{\sigma}_{\text{LN}}(T_{i-1}), T_{i-1}, K, (T_{i-1} - t)P(t, T_i)\right), \tag{3.13}$$

and

$$V^{\text{Caplet}}(t) = V_{\text{Bachelier}}(F(t; T_{i-1}, T_i), \tilde{\sigma}_{\text{N}}(T_{i-1}), T_{i-1}, K, (T_{i-1} - t)P(t, T_i)). \tag{3.14}$$

[4] One could also deploy the shifted lognormal, CEV or SABR models.

[5] Modelling the forward rate is a different approach to modelling the short rate as we have considered in this dissertation. We only consider the forward-rate models for the purposes of implied volatility.

We make use of the following algorithms to generate model-implied volatility:

Algorithm 2 Lognormal \Normal model-implied volatility $\tilde{\sigma}_{\text{LN}}$ \$\tilde{\sigma}_{\text{N}}$ for a Caplet for a fixed maturity T_{i-1}: $(T_{i-1}, K) \mapsto \sigma_{\text{LN}}(T_{i-1}, K)$ \$\sigma_{\text{N}}(T_{i-1}, K)$

.

for Each K, **do**

1. Given strike K, calculate the FD caplet price
2. Using the FD scheme, obtain bond prices $P(t, T_{i-1})$ and $P(t, T_i)$
3. Calculate the model-implied simple forward-term rate using (3.10)
4. Obtain lognormal model-implied volatility by inverting Black's \Bachelier's formula (3.13)

end for

Next K

3.3.1 Reconciliation of lognormal model-implied volatility with normal model-implied volatility

Let σ_{LN}, F, K, and τ denote the lognormal volatility, forward price, strike price, and time to maturity, respectively. Choi *et al.* (2022) provide an approximate relationship for converting lognormal volatility to normal volatility in (3.15):

$$\sigma_N \approx \sigma_{LN} F \sqrt{\frac{K}{F}} \left(\frac{1 + \frac{1}{24} \left(\log \frac{f}{K} \right)^2}{1 + \frac{\sigma_B^2 \tau}{24} \log \frac{f}{K}} \right). \tag{3.15}$$

In Section 4.2, we compute lognormal and normal implied volatilities using our finite-difference scheme, and we use (3.15) to reconcile them. Using the lognormal model-implied volatilities, we demonstrate that one can use (3.15) to recover normal model-implied volatilities.

Chapter 4

Results and analysis

In this section, we investigate the properties of the numerical implementation of our short-rate model (2.1). First, we plot bond and caplet prices as functions of the initial short-rate and time using Figure 4.1 and Figure 4.3. Then, we take cross-sections of those figures (Figure 4.2 and Figure 4.4) for a more detailed analysis. We then narrow our focus to caplets, presenting a reconciliation of caplet prices generated by our closed-form solution, Monte-Carlo and finite-difference framework. In general, we observe a relatively good fit; thus, we dispense with Monte-Carlo in later figures and rely solely on the results from the finite-difference scheme when we construct volatility skews. We show how varying jump parameters impact the volatility skew and caplet prices across various strikes using Algorithm 1 and Algorithm 2, and several iterations of the finite difference scheme outlined in Chapter 3. We then use (3.15) to approximate normal implied volatilities from the lognormal model-implied volatilities.

Table 4.1a, Table 4.1b and Table 4.1c outline the baseline parameters used throughout this section. All figures to come will assume these parameters unless otherwise specified.

Tab. 4.1: Base parameter set

(a) Factor jump model

κ	0.2
θ	0.05
σ_r	0.025
μ	0
$\mathcal{T}_J$	{0.25, 0.5, 0.75}

(b) Finite-difference

M	100
N	80
r_0	0
r_M	0.1

(c) Monte-Carlo

Number of paths	50000

4.1 Numerical reconciliation of the pricing equation

We first consider a zero-coupon bond with maturing in one year. Figure 4.1 depicts continuously-compounded[1] bond yields as a function of the initial short-rate r and time t. We then plot its cross-section across yield and initial short-rate in Figure 4.2, where we plot its bond yields with those given by Kim and Wright (2014) and the Monte-Carlo procedure defined in Section 3.2.

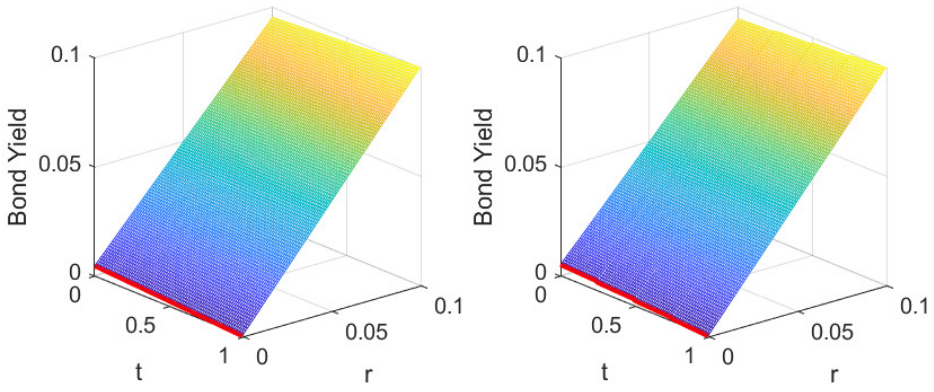

Fig. 4.1: Bond yields as a function of the initial short-rate r and time t. Left: Volatility and jump parameters $\alpha = \beta = \sigma_J = 0$; Right: Volatility and jump parameters $\alpha = \beta = 0$, $\sigma_J = 0.02$.

We consider a '9x12' caplet (with $T = 0.75$ and $S = 1$) with quarterly jumps. Figure 4.3 depicts caplet prices as a function of the initial short-rate r and time t. We then plot its cross-section across price and initial short-rate using the cross-section across caplet prices and the initial short-rate, and we reconcile caplet prices computed from our finite-difference scheme with a Monte-Carlo benchmark.

[1] Where yields are computed as follows, $y(t,T) = -\dfrac{\log\left(P(t,T)\right)}{T-t}$.

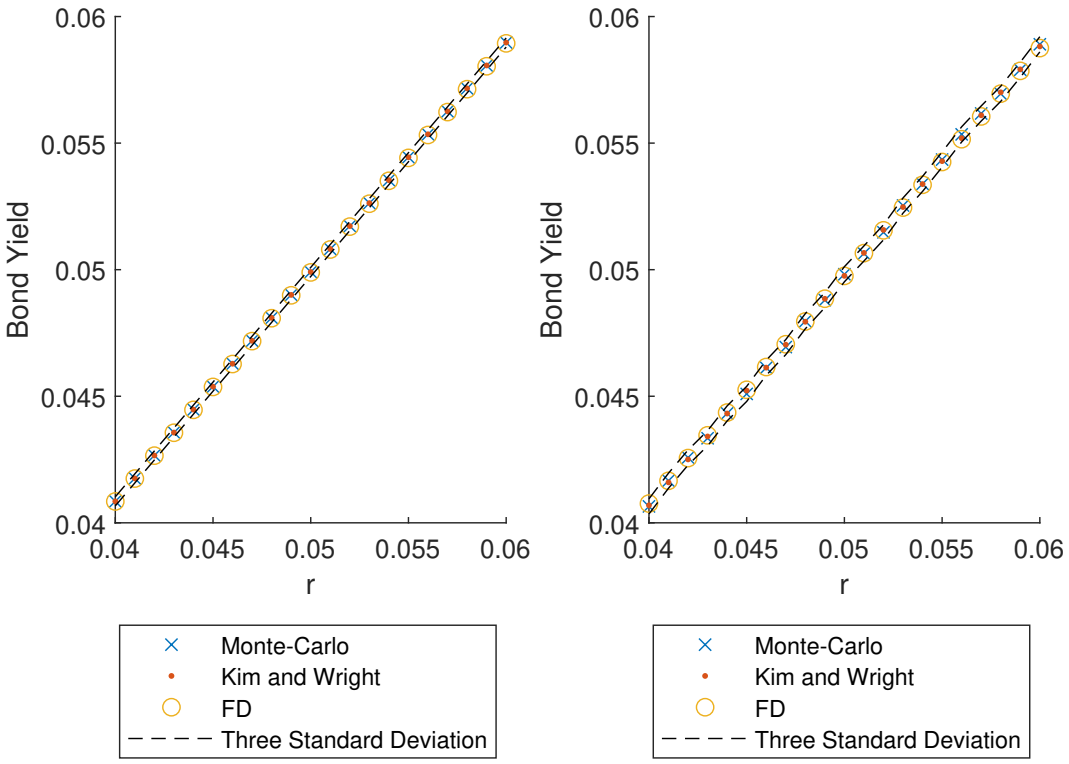

Fig. 4.2: Bond yields as a function of the initial short-rate r at time $t = 0$. Left: Volatility and jump parameters $\alpha = \beta = \sigma_J = 0$; Right: Volatility and jump parameters $\alpha = \beta = 0$, $\sigma_J = 0.0075$.

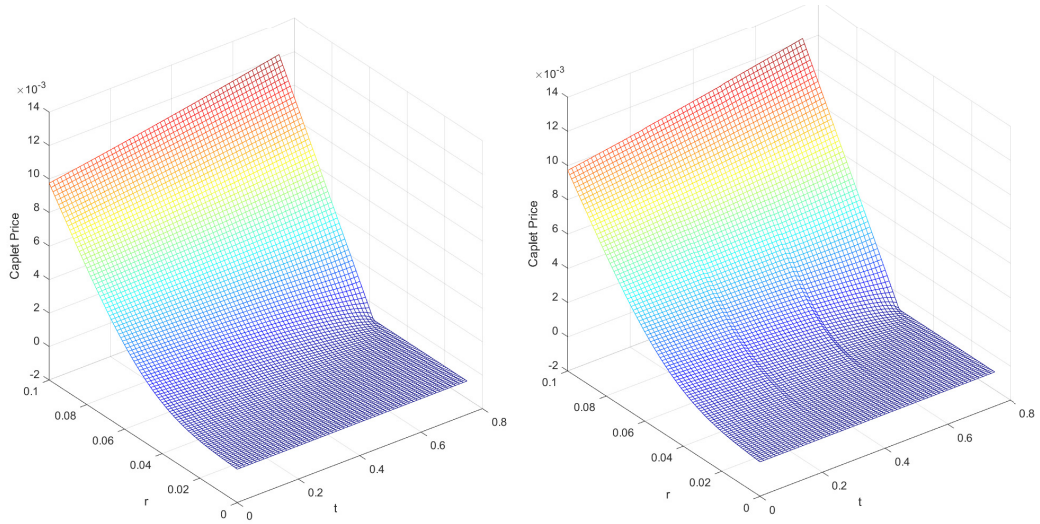

Fig. 4.3: Caplet prices as a function of initial short-rate r and time t. Left: Volatility and jump parameters $\alpha = \beta = \sigma_J = 0$; Right: Volatility and jump parameters $\alpha = 1$, $\sigma_J = 0.0075$, $\beta = 0$.

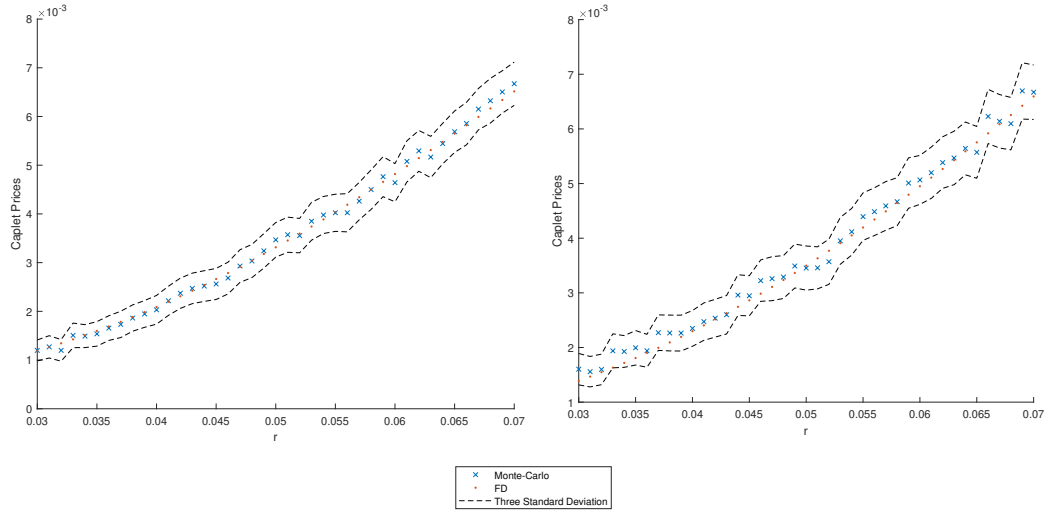

Fig. 4.4: Caplet prices as a function of initial short-rate r at time $t = 0$. Left: Volatility and jump parameters $\alpha = \beta = \sigma_J = 0$; Right: Volatility and jump parameters $\alpha = 1$, $\sigma_J = 0.0075$, $\beta = 0$.

4.2 Model-implied volatility and caplet price analysis

The ensuing analysis demonstrates the effect of each parameter in (2.1) on implied volatility and caplet prices. In addition to Table 4.1a, Table 4.1b and Table 4.1c, we assume the following caplet parameters in Table 4.2 below:

'9x12' caplet parameters							
t	0						
T	0.75						
S	1						
$r(0)$	0.05						
$F(t;T,S)$	0.0484						
K_i	K_1	K_2	K_3	K_4	K_5	K_6	K_7
	0.0184	0.0284	0.0384	0.0484	0.0584	0.0684	0.0784
Monte-Carlo parameters							
Number of paths	50000						

Tab. 4.2: '9x12' caplet parameters.

Recalling our discussion in Section 3.1.1, we obtain time-$t = 0$ caplet prices by first running (3.5) from time $t = S$ to time $t = T$ with $H = 1$ to price a zero-coupon bond. We obtain the forward rate (3.10) by running our finite difference scheme for

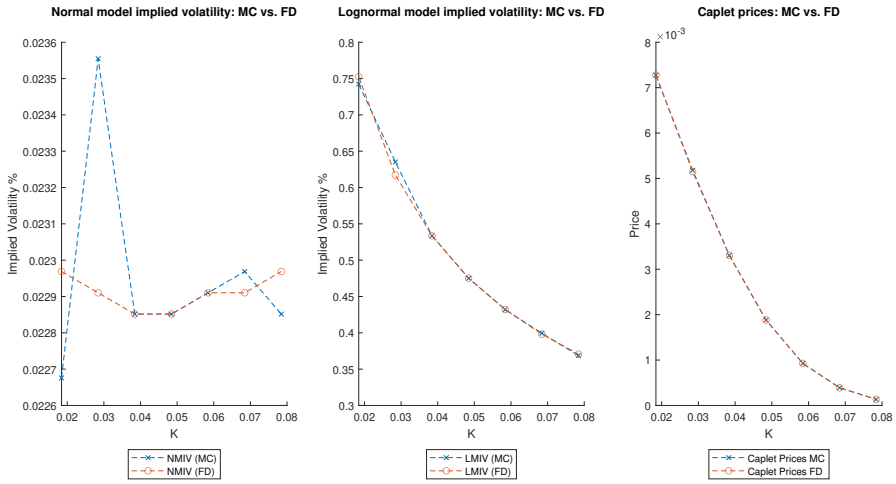

Fig. 4.5: Monte-carlo and finite-difference comparison of LMIV (first plot) and NMIV (second plot) alongside caplet prices (third plot).

zero-coupon bonds maturing at time $t = T$ and time $t = S$.

Figure 4.5 compares caplet volatility skews derived from our finite-difference scheme and Monte-Carlo procedure. Each panel above plots normal model-implied volatility, lognormal model-implied volatility and caplet prices across various strikes introduced in Table 4.2. In general, we observe an agreement between the two approaches; however, the left panel seems to indicate that the volatility skew generated from Monte-Carlo caplet prices has suffered from numerical precision.[2]

In Figure 4.6 and Figure 4.7, we show the results obtained by changing the parameter values for σ_r and σ_J. By increasing σ_r and σ_J, we observe a change in the level of the model-implied volatility skews. The skew constructed by the normal assumption for the forward rate is flat compared to its lognormal counterpart. At higher levels of σ_r and σ_J, we see higher caplet prices, which is expected since higher volatility might increase the likelihood of an underlying term rate rising to an in-the-money level.

Similarly, Figure 4.8 and Figure 4.9 show the results obtained by changing the parameter values for α and β. By increasing α and β, we observe a change in the magnitude of the slope of the model-implied volatility skew. For the caplet prices, we again observe a change in slope as both α and β increase, resulting in higher caplet prices. As outlined in Section 2.2, α and β aim to capture the magnitude of level-dependence; increases in the correlation between rates and their volatility can

[2] The vertical axis on the left panel of Figure 4.5 is zoomed in, i.e., the large spike is actually a small numerical error.

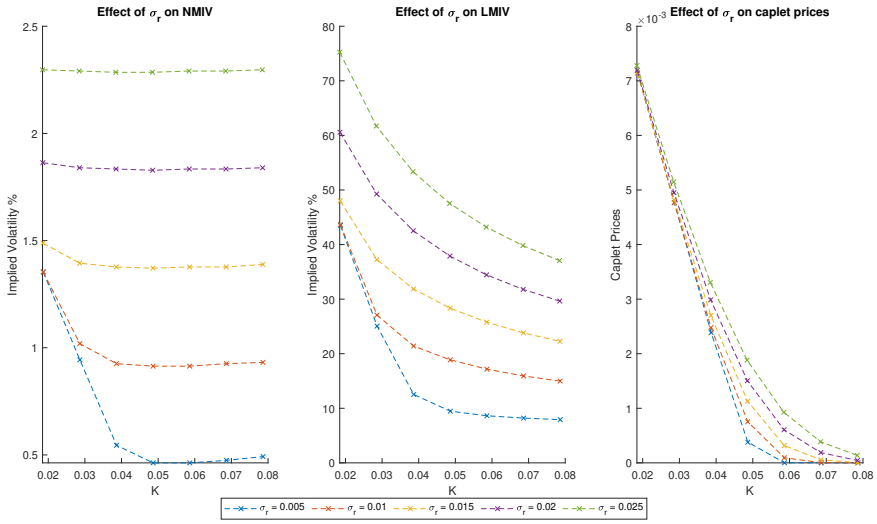

Fig. 4.6: Effect of changes in σ_r on NMIV (first plot) and LMIV (second plot) alongside caplet prices (third plot).

correspond to increases in positive level-dependence and subsequently increases in α and β, which result in higher caplet prices.

Figure 4.10 uses a result from Choi *et al.* (2022) to depict the relationship between normal and lognormal volatilities. The figure (3.15) reconciles our lognormal model-implied volatilities with our normal model-implied volatilities.

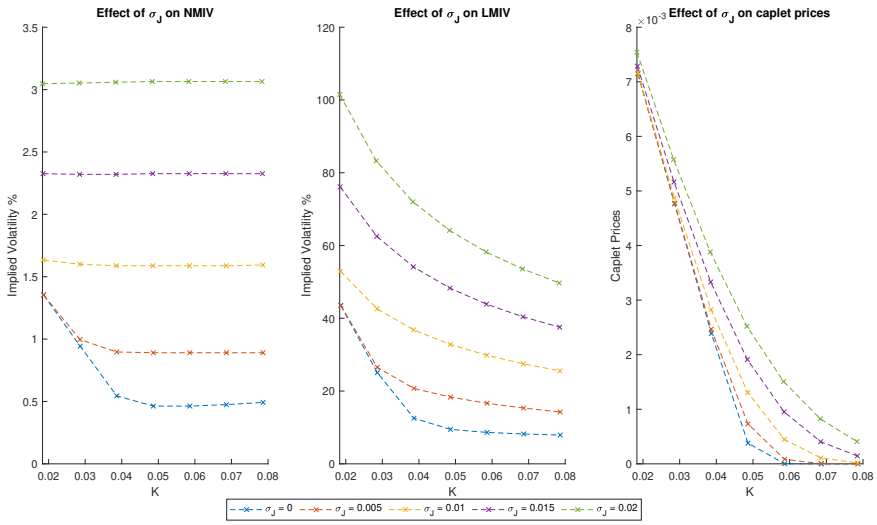

Fig. 4.7: Effect of changes in σ_J on NMIV (first plot) and LMIV (second plot) alongside caplet prices (third plot).

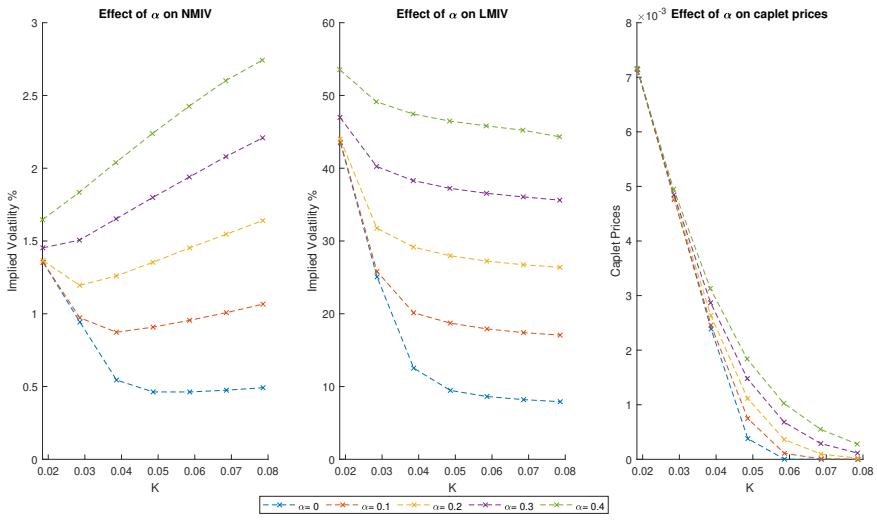

Fig. 4.8: Effect of changes in α on NMIV (first plot) and LMIV (second plot) alongside caplet prices (third plot).

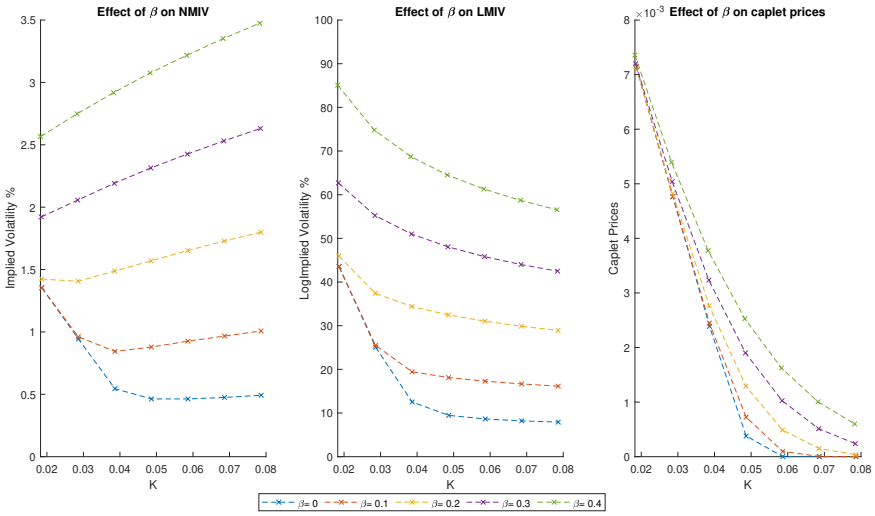

Fig. 4.9: Effect of changes in β on NMIV (first plot) and LMIV (second plot) alongside caplet prices (third plot).

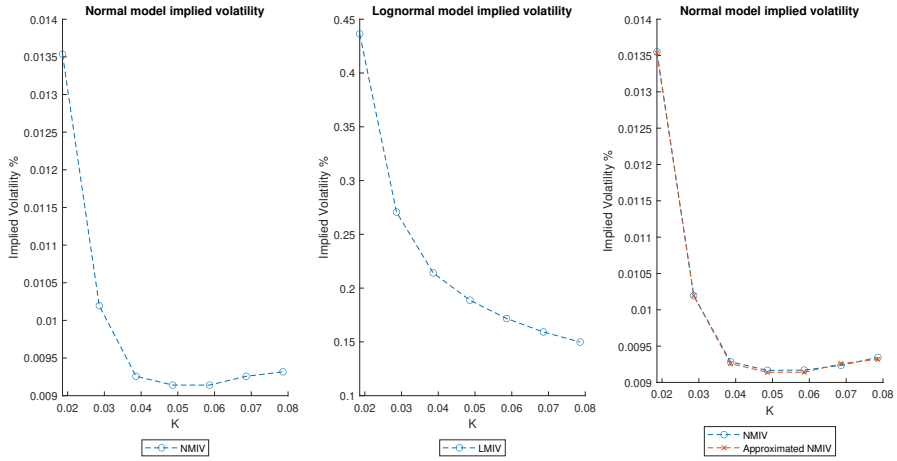

Fig. 4.10: Reconciliation of FD NMIV with Choi *et al.*'s approximation.

Chapter 5

Conclusion

The framework developed in this dissertation allows one to price interest rate contingent claims through finite-difference methods in a setting where jumps are expected to occur at known times (corresponding to macroeconomic announcements and other sudden developments).

Through volatility level-dependence, we have proposed an extension to the model used by the Kim and Wright (2014) model with deterministic jumps. The primary goal of this model was to observe the impact on the volatility skew given varying gradations of volatility level-dependence. At different specifications of level-dependence, we saw the model's ability to generate different shapes for the volatility skew.

We find that at higher specifications of volatility level-dependence, the lognormal and normal volatility skew begin to slope upwards, corroborating the notion that interest rate volatility increases as increase rates increase. With the economic interpretation that level-dependence can capture market sentiment, views and uncertainty, we saw that this resulted in higher caplet prices being produced by our model.

This approach can be extended to account for unexpected jumps, multiple state variables and multiple curves (Backwell and Hayes, 2022). The numerical implementation accuracy could be improved by using the Crank-Nicholson method (Courtadon, 1982) and an adaptive mesh (da Silva *et al.*, 2016).

Future work can consider calibration to market data and fitting an initial term structure, and the model can then be assessed according to how well it can replicate volatility skews and surfaces observed in the derivatives market.

Bibliography

Andersen, L. and Bang, D. R. A. (2020). Spike Modeling for Interest Rate Derivatives with an Application to SOFR Caplets, *ERN: Other Econometrics: Econometric & Statistical Methods - Special Topics* .

Bachelier, L. (1900). Théorie de la spéculation, *Annales scientifiques de l'École normale supérieure* **17**: 21–86.

Backwell, A. and Hayes, J. (2022). Expected and Unexpected Jumps in the Overnight Rate: Consistent Management of the Libor Transition, *Journal of Banking & Finance* **145**: 106669.
URL: *https://www.sciencedirect.com/science/article/pii/S0378426622002497*

Backwell, A. and Rudd, R. (2023). Throwing away a billion Yuan, Real or Rand: the cost of sub-optimal hedging in high interest-rate environments, *Applied Economics* **55**(18): 2060–2069.

Bank of England (2024). Monetary Policy, https://www.bankofengland.co.uk/monetary-policy. Accessed in January 2024.

Bauer, M. (2014). Nominal Interest Rates and the News, *Journal of Money, Credit, and Banking* . Forthcoming.
URL: *https://ssrn.com/abstract=1343865*

Baz, J. and Das, S. R. (1996). Analytical Approximations of the Term Structure for Jump-Diffusion Processes, *The Journal of Fixed Income* **6**(1): 78–86.
URL: *https://jfi.pm-research.com/content/6/1/78*

Black, F. (1976). The pricing of commodity contracts, *Journal of Financial Economics* **3**(1): 167–179.
URL: *https://www.sciencedirect.com/science/article/pii/0304405X76900246*

Choi, J., Kwak, M., Tee, C. W. and Wang, Y. (2022). A Black–Scholes user's guide to the Bachelier model, *Journal of Futures Markets* **42**(5): 959–980.
URL: *http://dx.doi.org/10.1002/fut.22315*

Courtadon, G. (1982). A More Accurate Finite Difference Approximation for the Valuation of Options, *The Journal of Financial and Quantitative Analysis* **17**(5): 697–703.
URL: *http://www.jstor.org/stable/2330857*

Cox, J. C., Ingersoll, J. E. and Ross, S. A. (1985). A Theory of the Term Structure of Interest Rates, *Econometrica* **53**(2): 385–407.

da Silva, A. J., Baczynski, J. and Vicente, J. V. (2016). A new finite difference method for pricing and hedging fixed income derivatives: Comparative analysis and the case of an Asian option, *Journal of Computational and Applied Mathematics* **297**: 98–116.
URL: *https://www.sciencedirect.com/science/article/pii/S037704271500535X*

Das, S. R. (1996). Discrete-time bond and option pricing for jump-diffusion processes, *Review of Derivatives Research* **1**(3): 211–243.
URL: *https://doi.org/10.1007/BF01531143*

Duffie, D. and Kan, R. (1996). A yield-factor model of interest rates, *Mathematical Finance* **6**(4): 379–406.
URL: *https://onlinelibrary.wiley.com/doi/abs/10.1111/j.1467-9965.1996.tb00123.x*

Glasserman, P. (2003). *Monte Carlo Methods in Financial Engineering*, Springer New York, New York, NY, chapter 3, pp. 79–184.
URL: *"https://doi.org/10.1007/978-0-387-21617-1_3"*

Johannes, M. (2004). The statistical and economic role of jumps in continuous-time interest rate models, *The Journal of Finance* **59**(1): 227–260.
URL: *http://www.jstor.org/stable/3694895*

Kim, D. H. and Wright, J. H. (2014). Jumps in bond yields at known times, *Working Paper 20711*, National Bureau of Economic Research.
URL: *http://www.nber.org/papers/w20711*

Lyashenko, A. and Mercurio, F. (2019). Looking Forward to Backward-looking Rates: A Modeling Framework for Term Rates Replacing LIBOR.
URL: *https://ssrn.com/abstract=3330240*

Øksendal, B. (2003). *Stochastic Differential Equations: An Introduction with Applications*, Springer Berlin Heidelberg, Berlin, Heidelberg, chapter 8, pp. 141–180.
URL: *https://doi.org/10.1007/978-3-642-14394-6_8*

Piterbarg, V. (2020). Interest Rates Benchmark Reform and Options Markets, *SSRN Electronic Journal* .

Rebonato, R. (1996). *Interest-rate option models: understanding, analysing and using models for exotic interest-rate options*, Wiley, chapter 1, pp. 15–21.

Rebonato, R. (2004). *Volatility and Correlation: The Perfect Hedger and the Fox*, John Wiley & Sons, Ltd, chapter 7, pp. 201–235.
URL: *https://onlinelibrary.wiley.com/doi/abs/10.1002/9781118673539.ch7*

Schrimpf, A. and Sushko, V. (2019). Beyond LIBOR: a primer on the new benchmark rates, *BIS Quarterly Review* .
URL: *https://ideas.repec.org/a/bis/bisqtr/1903e.html*

Vasicek, O. A. (1977). An equilibrium characterization of the term structure, *Journal of Financial Economics* **5**: 177–188.

Appendix A

Representing caplets as a multiple of zero-coupon bond puts

Proposition A.1. *The time-T_i payoff of a caplet on a future term rate $L(T_{i-1}, T_i)$ (fixing at T_{i-1}), strike rate K and accrual period $[T_{i-1}, T_i]$ can be decomposed into a put on zero-coupon bond with strike P_K:*

$$\textit{Payoff}_{\textit{Caplet}} = (1 + K(T_i - T_{i-1}))\textit{max}(P_K - P(T_{i-1}, T_i), 0)$$

Proof. Given the payoff of a caplet at time T_i on a future term rate $L(T_{i-1}, T_i)$, with accrual period $\delta_i = T_i - T_{i-1}$, paying $\delta_i \text{max}(L(T_{i-1}, T_i) - K, 0)$

$\text{Payoff}_{\text{Caplet}} = \delta_i \text{max}(L(T_{i-1}, T_i) - K, 0)$

Discounting this payoff to time T_{i-1} yields:

$$\begin{aligned}
\frac{\text{Payoff}_{\text{Caplet}}}{1 + \delta_i L(T_{i-1}, T_i)} &= \frac{\delta_i \text{max}\left(L(T_{i-1}, T_i) - K, 0\right)}{1 + \delta_i L(T_{i-1}, T_i)} \\
&= \frac{\max\left(\delta_i (L(T_{i-1}, T_i) - K), 0\right)}{1 + \delta_i L(T_{i-1}, T_i)} \\
&= \frac{\max\left(\delta_i L(T_{i-1}, T_i) - \delta_i K, 0\right)}{1 + \delta_i L(T_{i-1}, T_i)} \\
&= \frac{\max\left(\delta_i L(T_{i-1}, T_i) + 1 - 1 - \delta_i K, 0\right)}{1 + \delta_i L(T_{i-1}, T_i)} \\
&= \max\left(\frac{1 + \delta_i L(T_{i-1}, T_i)}{1 + \delta_i L(T_{i-1}, T_i)} - \frac{1 + \delta_i K}{1 + \delta_i L(T_{i-1}, T_i)}, 0\right) \\
&= \max\left(1 - \frac{1 + \delta_i K}{1 + \delta_i L(T_{i-1}, T_i)}, 0\right) \\
&= (1 + \delta_i K)\text{max}\left(\frac{1}{1 + \delta_i K} - \frac{1}{1 + \delta_i L(T_{i-1}, T_i)}, 0\right) \\
&= (1 + \delta_i K)\text{max}\left(P_K - P(T_1, T_2)\right)
\end{aligned}$$

□

Appendix B

Abbreviations and notation

- BoE = Bank of England
- EBO = European Bond Option
- FD = Finite Difference
- KW = Kim-Wright
- LMIV = Lognormal Model Implied Volatility
- MC = Monte Carlo
- NMIV = Normal Model Implied Volatility
- OIS = Overnight-Index Swap
- RFR = Risk-free Reference Rate
- SONIA = Sterling Overnight Index Average
- ZCB = Zero-coupon Bond
- $\mathbb{E}^{\mathbb{Q}}$: Expectation under the risk-neutral measure $\mathbb{Q}$
- $\mathbb{1}_X$: Indicator function over a set X
- $\mathcal{N}(\mu, \sigma)$: Normal distribution with mean μ and standard deviation σ
- Φ: Cumulative distribution function of a standard normal distribution
- ϕ_X: Density function of a normally distributed random variable X